Published in final edited form as:

Adv Healthc Mater. 2020 February ; 9(4): e1901399. doi:10.1002/adhm.201901399.

Distinguishing Specific CXCL12 Isoforms on Their Angiogenesis and Vascular Permeability Promoting Properties

Chia-Wen Chang[1], **Alex J. Seibel**[1], **Alex Avendano**[2], **Marcos Cortes-Medina**[2], **Jonathan W. Song**[3,4,†]

[1]Department of Chemical and Biomolecular Engineering, The Ohio State University, Columbus, OH, USA

[2]Department of Biomedical Engineering, The Ohio State University, Columbus, OH, USA

[3]Department of Mechanical and Aerospace Engineering, The Ohio State University, Columbus, OH, USA

[4]The Comprehensive Cancer Center, The Ohio State University, Columbus, OH, USA

Abstract

Angiogenesis is known to be associated with increased vessel sprouting and permeability. Important mediators of these angiogenic responses include local biomolecular environment of signaling molecules and supporting extracellular matrix (ECM). However, dissecting the interplay of these instructive signals *in vivo* with multiple cells and extracellular molecules remains a central challenge. Here, we integrated microfluidic biomimicry to reconstitute vessel-like analogues *in vitro* with 3-D ECM hydrogels that were well-characterized for molecular-binding and mechanical properties. Our study focused on three distinct isoforms of the pro-metastatic chemokine CXCL12. In collagen-only hydrogel, CXCL12-α was the most potent isoform in promoting sprouting and permeability, followed by CXCL12-β and CXCL12-γ. Strikingly, addition of hyaluronan (HA), a large and negatively-charged glycosaminoglycan, with collagen matrices selectively increased the vessel sprouting and permeability conferred by CXCL12-γ. This outcome was supported by the measured binding affinities to collagen/HA ECM, suggesting that negatively-charged HA increased the binding of CXCL12-γ to augment its angiogenic potency. Moreover, we show that addition of HA to collagen matrices on its own decreased vessel sprouting and permeability, and these responses were nullified by blocking the HA receptor CD44. Collectively, our results demonstrate that differences in binding to HA help underlie CXCL12 isoform-specific responses towards directing angiogenesis.

Keywords

Extracellular matrix; hyaluronic acid; microvessel analogue; microfluidics; vascular function; matrix-bound ligands; chemokine

[†]Correspondence to: song.1069@osu.edu.

Conflicts of Interest

The authors declare that they have no competing interests.

1. Introduction

Expansion of the pre-existing blood vasculature is known as angiogenesis[1], and is often affected by or engaged in pathologies such as cancer, atherosclerosis, and chronic inflammation[2]. Pathological angiogenesis results in excessive formation of new, unstable, permeable, and poorly functioning blood vessels that further promotes disease progression[3]. Chronic vessel permeability can also lead to elevated interstitial fluid pressure (or hydrostatic edema), which has deleterious effects on tissue function by impeding both mass (e.g. oxygen and nutrients) and drug transport[4]. In addition, a leaky vasculature may facilitate leukocyte infiltration that can exacerbate edema[5], or escape of tumor cells leading to distant metastases [6]. Therefore, there is great interest in health and disease in understanding the important aspects of vascular biology that regulate angiogenesis and vessel permeability.

Central to angiogenesis and vessel permeability is the coordinated morphological responses by vascular endothelial cells to a myriad of instructive signals or cues[7]. Examples of these cues include physical interactions with the extracellular matrix (ECM) and biochemical signaling through both soluble (i.e. freely diffusing) and insoluble (i.e. matrix-bound) ligands such as growth factors, chemokines, and inflammatory cytokines[8]. Under normal physiological conditions, the pro- and anti-angiogenic signals are appropriately balanced such that the vasculature is stable and the vessel barrier function is well controlled. However, this important balance is lost during pathological progression[9]. In the context of tumors, dysregulated ECM composition and architecture is a hallmark of cancer[10]. For instance, the elevated ratio of fibrillar collagen (e.g. type I and type III) and certain non-fibrillar components such as hyaluronan (HA), a non-sulfated and negatively charged glycosaminoglycan (GAG) molecule[11], is characteristic of aggressive or desmoplastic tumors[12]. This characteristic of the tumor ECM also leads to stiffer tissue and a subsequent self-sustaining and persistent feed-forward loop for tumor cell growth, survival, migration, epithelial-to-mesenchymal transition (EMT)[13], and a tumor vessel phenotype[14]. However, changes in ECM content in tumors also augment the capacity to sequester growth factors and signaling molecules in a way that increases local concentrations and subsequently the tumor-promoting potency of ligand molecules. Therefore, understanding how physical alterations to the tumor ECM interplays with the local biochemical environment, is necessary to improve cancer detection, prevention, and treatment.

A key example of this physicochemical regulation in tumor ECM involves the chemokine C-X-C motif chemokine ligand 12 (CXC12, also known as stromal cell-derived factor −1 or SDF-1). CXCL12 is secreted by cancer associated fibroblasts (CAFs) at the primary tumor site to stimulate tumor growth[15], angiogenesis[16], and tumor cell intrasvasation[17]. Like many other important cytokines in cancer (e.g. VEGF and TGF), there are multiple isoforms of CXCL12 formed by alternative splicing. Humans have three major CXCL12 isoforms (α, β, γ) with distinct structural and biochemical functionality[18]. However, studies of CXCL12 typically focus on CXCL12-α, which has the strongest binding affinity for the CXCL12 cognate receptor CXCR4, followed by the β and then γ isoform[19]. Compared to CXCL12-α, CXCL12-β and CXCL12-γ add three and 18 additional positively-charged amino acids to the C-terminus[19] respectively, which confers increased binding to negatively charged GAG

molecules such as heparan sulfate (HS) and HA, with the γ isoform exhibiting one of highest known binding affinities for HS (1.5 nM)[19]. In addition, it was confirmed recently using genetically engineered mice the necessity of CXCL12/HS binding for angiogenesis during skeletal muscle regeneration[20].

In a recent study by Connell et al., it was reported that when CXCL12-γ was presented with HS to CXCR4-expressing cells *in vitro*, the signaling and chemotactic responses were similar to that elicited by CXCL12-α alone. The results from this study suggested that negatively charged GAG molecules such as HS help control CXCL12 activity in an isoform-specific manner. In another study by Ray et al., it was shown using *in vivo* mouse models that the γ isoform of CXCL12 most potently drives breast cancer metastasis at the primary site[21]. One possible explanation for CXCL12-γ promoting metastasis *in vivo* despite its relative low binding affinities for CXCR4 may be attributed to its C-terminal being enriched with positively charged basic residues that enhance electrostatic binding and immobilization to negatively charged matrix proteins to generate migration-inducing gradients from the ECM, even at low total abundance[22]. However, to our knowledge, it has not been confirmed experimentally if the composition of the ECM helps determine the angiogenesis responses conferred by different CXCL12 isoforms.

The present study seeks to elucidate how altering the ECM influence angiogenesis and vascular permeability responses by three different CXCL12 isoforms (α, β, γ) (Figure 1A). Using a biomimetic microfluidic microvessel analogue to systematically measure sprouting angiogenesis and vascular permeability, we observed that CXCL12-α most potently promotes both sprouting and vessel permeability in the presence of ECM comprised of Type I collagen-only. However, the addition of HA to collagen matrices specifically enhances the sprouting and vascular permeability responses of CXCL12-γ only. Moreover, we verified with surface plasmon resonance (SPR) that CXCL12-γ exhibited significantly increased binding to collagen/HA surfaces compared to the α and β isoforms. In contrast, there were no CXCL12 isoform specific differences in binding to collagen-only surfaces. Furthermore, our finding also shows that addition of HA to collagen matrices on its own decreased vessel sprouting and permeability. These results suggest that differences in HA binding by CXCL12 isoforms helps underlie their angiogenic potency. Collectively, our study demonstrates that the composition of the ECM mediates specific matrix-ligand binding interactions that control angiogenesis and vascular permeability phenotypes.

2. Experimental Results

2.1 Microfluidic device and ECM characterization.

A biomimetic microfluidic microvessel analogue system was fabricated using poly(dimethylsiloxane) (PDMS) soft lithography to study the effect of CXCL12 isoforms on angiogenesis, and the modulation by specific ECM components. The microfluidic device contained three parallel channels (Figure 1B). The two outer channels were lined with human umbilical vein endothelial cells (HUVECs) to form microvessel analogues[23] (Figure 1C). The central channel in between and laterally adjacent to the microvessel analogues formed a 3-D ECM compartment that was comprised either of Type I collagen gel alone (henceforth referred to as “collagen-only”) or a mixture of Type I collagen gel and

high molecular weight HA (Sigma)[24] (henceforth referred to “collagen/HA”). For Type I collagen gel constituent, either 3 or 6 mg/mL concentrations were employed to conduct the sprouting angiogenesis assay and vessel permeability measurement respectively. These concentrations for the collagen gel constituent were used for both the collagen-only and the collagen/HA conditions. For collagen/HA conditions, HA at a concentration of 1 mg/mL was mixed with collagen gel prior to polymerization. Previous reports on the ratio of collagen to HA in breast tumors *in vivo* range from 2.4:1 – 7.7:1[25]. Therefore, the collagen to HA ratios used for this study (3:1 for the 3 mg/mL collagen condition and 6:1 for the 6 mg/mL collagen condition) are in line with these previously reported results.

The importance of mechanical properties of the ECM in tumor progression is now well accepted[26]. Thus, we characterized the mechanical stiffness of different ECM compositions that were reconstituted *in vitro* using a high precision mechanical indentation testing system for hydrogels (TA Instruments, Electroforce 5500). The measured stiffness for 3 mg/mL collagen-only gels was 2.65 kPa (Figure 1D). Addition of HA at a concentration of 1 mg/mL to 3 mg/mL collagen gels significantly increased the ECM stiffness to 4.51 kPa. At 6 mg/mL, the stiffness of the collagen-only gels were measured to be 8.75 kPa. Addition of HA at a concentration of 1 mg/mL to 6 mg/mL collagen gels significantly increased ECM stiffness to 17.81 kPa. For physiological context, the stiffness profile for normal breast tissue is ~3 kPa[27] while the previously reported range of stiffness measurements for breast cancer tissue is 10.0–42.0 kPa[27b]. Collectively, these results confirm that at a fixed collagen concentration, the addition of HA enhances the mechanical stiffness of the ECM, as measured by indentation testing[28].

In addition to characterizing the stiffness profiles of the ECM mixtures, we measured the binding affinity of the CXCL12 isoforms (α, β, γ) onto ECM surfaces using a surface plasmon resonance (SPR) based assay[29]. For this assay, we measured the equilibrium absorption of each CXCL12 isoforms onto the collagen-only (6 mg/mL) or collagen/HA (6 mg/mL collagen and 1 mg/mL HA) ECM surfaces that were cast on proprietary SPR chips (Nicoya technology) and polymerized overnight. Each CXCL12 isoform (100 ng/mL) was incubated onto ECM-treated surfaces for 1 day and measured with a Nicoya LSPR instrument[30]. The peak intensity of each sample’s absorbance spectrum was considered the equilibrium absorption. For each experimental measurement, we measured the absorbance intensity of an untreated surface to serve as an internal normalizing factor. Our results demonstrated no significant difference among the CXCL12 isoforms in binding to the collagen-only surface (Figure 2A). This outcome suggests that CXCL12 isoforms bind indiscriminately to collagen-only ECM. In contrast, for collagen/HA surfaces, CXCL12-γ exhibited significant increased binding by 7% to compared to the α and β isoforms (Figure 2B). These results demonstrate that altering the ECM content through the addition of negatively-charged HA to the collagen ECM mixture preferentially enhances the binding of the more positively-charged γ isoform versus the α and β isoforms.

2.2 Sprouting angiogenesis mediated by CXCL12 isoforms is contingent on ECM composition.

We first assessed the angiogenesis promoting properties of specific CXCL12 isoforms using our HUVEC-lined microvessel analogue system containing either collagen-only (3 mg/mL) or collagen/HA (3 mg/mL collagen, 1 mg/mL HA) 3-D ECM gels. The microvessels were treated with individual CXCL12 isoforms and compared to untreated controls by measuring the normalized sprouting percentage (see Materials and Methods) for the experimental conditions. In the collagen-only ECM, the untreated controls demonstrated minimal sprouting (0.15% on day 1 and 0.78% at day 3), as expected (Figure 3A). In contrast, CXCL12-α treatment elicited the greatest normalized sprouting percentage response in the collagen-only ECM, increasing from 1.72% at day 1 to 4.29% at day 3. For comparison, the normalized sprouting percentage showed no significant difference for CXCL12-β and CXCL12-γ in collagen-only ECM at day 3, which was 1.65% and 1.02% respectively. Therefore, in the collagen-only ECM, the rank order for the angiogenesis potency by the CXCL12 isoforms was α > β > γ. In addition, the sprout morphologies in response to different CXCL12 isoforms are also shown in Figure 3A.

The normalized sprouting percentage for CXCL12 isoform-treated microvessels into a collagen/HA ECM are shown in Figure 3B. Similar to the collagen-only ECM, untreated microvessels demonstrated low levels of sprouting in the collagen/HA ECM (0.22% sprouting ratio at day 3). Interestingly, of the three isoforms tested, CXCL12-γ elicited the most potent sprouting response in the collagen/HA ECM, increasing from 0.69 % at day 1 to 1.69 % at day 3. For comparison, there was no significant difference in normalized sprouting percentage for CXCL12-β (1.04%) and CXCL12-α (0.74%) in collagen/HA ECM at day 3. These vessel sprouting results were supported by the demonstrated CXCL12-isoform specific responses of the SPR binding assay where the addition of negatively charged HA to collagen ECM specifically enhanced the electrostatic interactions and immobilization of CXCL12-γ (Figure 2). Therefore, the collagen/HA mixture provides a binding surface that augments the signaling response of CXCL12-γ to the microvessel analogues. Consequently, the rank order for the angiogenesis potency of the CXCL12 isoforms was inverted to γ > β > α for the collagen/HA ECM compared to the collagen-only ECM.

In addition, we observed distinct vessel morphologies in response to treatment by individual CXCL12 isoforms in the collagen-only and collagen/HA devices. For the collagen-only ECM, treatment with each of the CXCL12 isoforms resulted in multicellular extensions or sprouts from the endothelial layer at the vessel/ECM interface (Figure 3A). In contrast, for the collagen/HA ECM, treatment with the individual CXCL12 isoforms promoted sheet-like migration of the endothelial cells that was reminiscent of local vessel dilation[31] (Figure 3B). We further characterized this vessel dilation response by analyzing the total area displacement of the HUVEC monolayer into the collagen/HA ECM during the course of the experiments (Figure S1). We observed that the CXCL12-γ treated microvessels showed significantly more vessel dilation (3740 μm^2), as measured by the total displacement area of HUVECs, compared to both CXCL12-β (1622 μm^2) and CXCL12-α (1317 μm^2) treated microvessels (Figure S1). It is well-established that tumor blood vessels are more dilated and leaky compared to normal vessels[32]. Therefore, the observed outcomes suggest that

collagen/HA matrices combined with CXCL12 treatment can promote a tumor angiogenesis phenotype.

2.3 HA stabilizes vessel barrier function yet specifically enhances permeability by CXCL12-γ.

Typically, elevated vessel permeability is a consequence or either an acute or chronic pathophysiological insult (e.g. inflammation or cancer) and is also coincident with increased angiogenesis[1]. Therefore, we evaluated whether altering the ECM content can impact the potency of different CXCL12 isoforms on vessel permeability when applied individually. We measured the apparent vascular permeability by tracking the transvascular transport of a fluorescent tracer dye conjugated to a macromolecule of known molecular weight dissolved in culture medium (see Materials and Methods). We note that for the vessel permeability assay, we increased our collagen working concentration from 3 mg/mL used for our sprouting assay to 6 mg/mL because this elevated collagen concentration eliminated significant sprouting that would disrupt our permeability measurements. In the collagen-only ECM, the average vessel permeability for the untreated control was 4.52×10^{-6} cm/s (Figure 4). Treatment with CXCL12-α in the collagen-only ECM more than doubled the vessel permeability to 1.29×10^{-5} cm/s. In contrast, treatment of the microvessels with CXCL12-β or CXCL12-γ had no significant effect and slightly decreased vessel permeability (3.10×10^{-6} cm/s and 2.86×10^{-6} cm/s respectively). These results demonstrate clearly that for collagen-only ECM, the α isoform was the most potent in increasing vessel permeability.

Next, we measured vessel permeability for collagen/HA ECM. For CXCL12-α treated microvessels, the vessel permeability decreased significantly for the collagen/HA ECM (6.43×10^{-6} cm/s) versus the collagen-only ECM (1.29×10^{-5} cm/s) (Figure 4). For CXCL12-β treated microvessels, there was no difference vessel permeability in the collagen/HA (3.37×10^{-6} cm/s) versus collagen-only (3.10×10^{-6} cm/s) matrices. Finally, for CXCL12-γ treated microvessels, the vessel permeability was significantly greater by 2.2-fold for the collagen/HA ECM (6.37×10^{-6} cm/s) versus the collagen-only ECM (2.86×10^{-6} cm/s). Therefore, addition of HA to the collagen ECM selectively increased the vessel permeability conferred by γ isoform compared to the collagen-only ECM, while having no effect for the β isoform, and decreasing permeability for the α isoform. Similar to the sprouting responses in the collagen/HA ECM, the vessel permeability results are supported by the demonstrated CXCL12-isoform specific responses of the SPR binding assay. These results suggest that altering the ECM composition can augment the capacity of the ECM to sequester growth factors which ultimately alter their signaling potency. An important regulator of endothelial barrier function is the adherens junction protein VE-cadherin[33]. We assessed interendothelial expression of VE-cadherin at the HUVEC/ECM interface. By visual inspection, there was no difference in cell coverage, cell morphology and expression of VE-cadherin between for the HUVECs grown on collagen-only versus collagen/HA ECM (Figure 4B and 4C).

2.4 Vessel sprouting and permeability mediated by the HA receptor CD44.

When comparing the untreated conditions, we observed that both vessel sprouting and permeability decreased significantly by 72% and 46% respectively for the collagen/HA

ECM versus the collagen-only ECM. Moreover, for the CXCL12- α conditions, there was also a similar suppression of vessel sprouting and permeability in the collagen/HA versus the collagen-only matrices, which decreased by 79% and 50% respectively. These results prompted us to investigate whether the differences in vessel sprouting and permeability were mediated by the HA receptor CD44[34], which has previously been shown to help regulate vascular barrier function[35]. To study this effect, we applied a blocking antibody for CD44 (Invitrogen, MA5–13890) and measured the vessel sprouting and permeability responses in the absence of CXCL12 treatment.

For the collagen-only ECM, anti-CD44 had no effect on the normalized sprouting percentage (0.74 % at day 3) compared to untreated microvessels (0.78%) (Figure 5A). As expected, these results support that the HA receptor CD44 is not involved with sprouting responses in collagen-only ECM. However, application of the CD44 blocking antibody significantly increased the sprouting percentage in the collagen/HA ECM (from 0.22% to 0.82 %). Therefore, in the collagen/HA ECM, blocking CD44 on HUVECs restores vessel sprouting to the levels observed for the collagen-only ECM (0.82 % versus 0.74 %). With regards to vessel permeability, for the collagen-only ECM, the anti-CD44 antibody had no significant effect, as expected (Figure 5B). In contrast, for the collagen/HA ECM, application of anti-CD44 increased the vessel permeability by ~35% from 2.43×10^{-6} cm/s to 3.35×10^{-6} cm/s. However, this increase was not statistically significant. Moreover, the vessel permeability for anti-CD44 treated microvessels was lower for the collagen/HA ECM (3.35×10^{-6} cm/s) versus collagen-only ECM (3.9×10^{-6} cm/s). Therefore, in the collagen/HA ECM, blocking CD44 on HUVECs only partially rescues the vessel permeability values to the levels observed for the collagen-only ECM.

3. Discussion

The pivotal role of CXCL12 in promoting tumor growth and metastasis from the primary site are well-established[15–17, 21, 36]. Yet, studies on CXCL12 typically focus on the α isoform or do not specify an isoform. Defining functions of specific isoforms of CXCL12, rather than considering this chemokine as a single entity, will advance understanding of CXCL12 in cancer and other diseases. Furthermore, the recent findings from *in vivo* settings that distinguish CXCL12 isoforms by their tumor promoting properties also demonstrate the heightened importance of assessing the cellular responses of CXCL12 isoforms in physiological-like settings that include 3-D ECM, which can preferentially augment the potency of the γ and β isoforms over the more well-characterized α isoform[22b]. However, the instability and heterogeneity of *in vivo* cancer can make it very difficult to experimentally manipulate and derive information on the CXCL12-mediated regulatory circuits on distinct compartments of tumors, such as the vasculature.

Here we integrated microfabrication to reconstitute vessel-like analogues *in vitro* with ECM hydrogels that were well-characterized by their mechanical and CXCL12-binding properties. This approach enabled us to precisely distinguish specific isoforms of CXCL12 on their angiogenesis and vascular permeability properties that were also mediated by changes to the ECM composition. In the collagen-only ECM, the rank order of the CXCL12 isoforms in promoting sprouting and permeability was α > β > γ. This order for angiogenic potency in

the collagen-only ECM mirrors the known binding affinities of these isoforms to the CXCR4 receptor[19]. It was previously reported that collagen binds weakly and indifferently to individual CXCL12 isoforms[22b], which was supported by our SPR results. Together, these previous reports with our findings demonstrate that when presented in its soluble form to endothelial cells, CXCL12-α is the most pro-angiogenic CXCL12 isoform.

A major finding of this study is the addition of HA to the collagen-based matrices specifically augments the angiogenic potency of CXCL12-γ. Angiogenesis can promote metastasis from the primary tumor site by providing a route for vascular intravasation[16]. A recent *in vivo* study defined stromal-originating CXCL12 in promoting vascular permeability that led to increased metastasis to distant sites[17]. While this study elegantly elucidated the cross-talk between the mammary stromal and endothelial compartments using a conditional knockout mouse, this model does not discern for individual CXCL12 isoforms. In another leading study that identified CXCL12-γ in primary tumors in driving breast cancer metastasis, the *in vivo* model used was an orthotropic xenograft where CXCR4-expressing cancer cells were co-implanted with fibroblasts that secreted individual isoforms of CXCL12 (α, β, or γ)[21]. An intriguing finding from this study was that while all CXCL12 isoforms produced comparable growth of mammary tumors, CXCL12-γ significantly increased metastasis to distant sites compared to the other isoforms. Our study isolated the effects of CXCL12 isoforms on the vasculature, and our findings suggest that CXCL12-γ promotes metastasis through the expansion of a leaky and dilated tumor vasculature in ECM containing both collagen and HA.

The physiological relevance of our findings is readily apparent because breast tumors are known to be especially rich in collagen and HA[37]. With regard to HA, it is believed to have both tumor-promoting and -suppressing properties[38]. Our results provide insights into the dual nature of HA. In contrast to our findings due to the combined effects of CXCL12-γ and HA, the addition of HA alone to collagen-based matrices suppresses angiogenesis and vessel permeability. However, the accumulation of HA specifically in the peritumoral stroma has been directly implicated in the distant metastasis of breast cancer[39]. In our study, CXCL12 was applied inside the microchannels lined with HUVECs (i.e. intravascularly) whereas in the tumor microenvironment *in vivo*, CXCL12 is most prominently secreted by stromal fibroblasts located outside of blood vessels (i.e. extravascularly). Thus, a possible interpretation of our findings is secreted CXCL12-γ from inside tumors that enters the tumor microcirculation is transported to the HA-rich peritumor stroma to help activate angiogenesis, vessel permeability, and distant metastasis at this location. Moreover, targeting CXCL12 by competitive inhibitors and the tumor ECM by enzymatic degradation have emerged as two essential therapeutic strategies of widespread interest and investigation[40]. Therefore, the findings from our study can be informative of how to optimize these strategies for inhibiting metastasis that is contingent for expression levels of CXCL12 isoforms and tumor ECM composition.

In addition to investigating the angiogenic effects of soluble and insoluble/matrix-bound CXCL12 isoforms, our study measured vascular outcomes due to ECM-specified HA and cell receptor CD44 interactions. The addition of HA to our collagen-based matrices suppressed both vessel sprouting and permeability in the absence of CXCL12 treatment.

Neutralizing HA-CD44 interactions with a blocking antibody for CD44 completely restored sprouting and partially rescued permeability levels compared to the collagen-only counterparts. These results support that CD44 is key for controlling HA-mediated angiogenic responses. Another manner by which HA alters the ECM is by increasing stiffness, which we measured for our ECM hydrogel mixtures using indentation testing. We confirmed that the stiffness profiles of the ECM hydrogel mixtures used for this study were in line with normal mammary and breast tumor tissues[27]. A recent study using matrix cross-linking showed that tissue stiffness promotes vessel outgrowth and decreased vessel barrier function[14]. However, our study, as was conducted, is not conducive for identifying stiffness-mediated angiogenesis because the HA-mediated increases in stiffness were also associated with increases in total ECM concentration. Therefore, our study does not decouple the effects of stiffness and ECM ligand functionality. Nonetheless, our findings demonstrate the multifaceted influence that ECM-specified HA can exert on vessel sprouting and permeability, whether acting directly through CD44 signaling or indirectly by sequestering and augmenting the potency of certain chemokines (e.g. CXCL12- γ).

4. Conclusion

Using 3-D microfluidic biomimicry, we investigated how the ECM-binding capabilities of specific CXCL12 isoforms (α, β and γ) influence vessel sprouting and permeability. As expected, CXCL12-α demonstrated to be the most potent of the isoforms tested in promoting sprouting angiogenesis and vessel permeability in collagen-only hydrogels. However, our findings demonstrate that the addition of HA to collagen-based hydrogels preferentially augments sprouting and permeability responses conferred by the γ isoform. Moreover, the increased potency of the γ isoform on angiogenic responses in collagen/HA may be attributed to matrix-ligand binding interactions that are not prominent in collagen-only ECM. This notion is supported by the measured binding affinities of the CXCL12 isoforms onto ECM surfaces, where we verified that CXCL12-γ exhibited significantly increased binding to the collagen/HA surface compared to the α and β isoforms. We also observed that HA on its own decreased vessel sprouting and permeability, and these responses were nullified by functional blocking the HA receptor CD44. Collectively, our results demonstrate that differences in binding to the ECM help underlie CXCL12 isoform specific-differences in angiogenesis. Furthermore, these findings were enabled by our deconstructed *in vitro* approach that integrated microfabrication with detailed ECM materials characterizations to advance our understanding of the CXCL12-ECM regulatory circuit that orchestrates angiogenesis.

5. Materials and Methods

5.1 Fabrication of microfluidic device

The biomimetic microfluidic microvessel analogue was fabricated using PDMS lithography. Briefly, the basic and curing agent of PDMS was mixed at 10:1 ratio and poured onto patterned mold wafer. Then, the patterned PDMS layer was irreversibly bonded onto a glass slide by plasma treatment. The assembled microfluidic device was placed in the 65°C overnight to promote the bonding between PDMS and glass slide. Type I collagen gel

(Corning Inc.) isolated from rat tail was introduced into the central compartment as the ECM component and polymerized at 37˚C in a humidified incubator overnight prior to cell seeding. High molecular weight HA was mixed with collagen gel at a concentration of 1 mg/mL HA to prepare collagen/HA matrices. The collagen-only or the collagen/HA pre-polymer mixture was pipetted into the central channel and polymerized overnight in an incubator before further usage.

5.2 Mechanical characterization of extracellular cellular matrices

Both 3 and 6 mg/mL concentration of collagen-only and collagen/HA were casted on 6 mm diameter custom made PDMS wells of 1 mm thickness. Samples were kept immersed in phosphate-buffered saline (PBS) during mechanical testing to maintain the collagen-based gels in a hydrated environment. Stiffness measurement was conducted by the high precision indentation system which was programmed to indent the gel to up to 40% strain at 10 % increasing intervals lasting 300 seconds each[41]. The peak loads responses were automatically recorded and used to calculate stress using the displacement at each interval and known indenter geometry (diameter of 4.8 mm). Stress responses were automatically recorded corresponding to each strain. The indentation modulus is defined as the ratio of stress over strain.

5.3 Preparation of HUVECs

Human umbilical vein endothelial cells (HUVECs) were purchased from Lonza and cultured in endothelial growth medium 2 (EGM-2) medium (Lonza). HUVECs were cultured in T-75 flasks in a humidified cell culture incubator at 37°C and 5 % CO_2 with the medium being changed every two days. Cell passage numbers of 5 – 12 were used in this study. To improve the biocompatibility of the microfluidic device, the lateral channels were coated with fibronectin solution at a concentration of 100 μg/mL at least 25 minutes prior to cell seeding. HUVECs were harvested from flasks using 0.05 % EDTA-Trypsin (Invitrogen) for 4 minutes, and the cell suspension was centrifuged at 950 RPM for 4 minutes. To acquire a monolayer of HUVECs lining the lateral channels, the cell suspension was adjusted to ~ 7×10^6 cells/mL and introduced to both channels by pipetting. Medium was changed every day in the device to ensure better cell attachment and healthy cell growth. For all experiments, treated conditions were introduced after cells had been cultured in the microfluidic device for 1 day to ensure treatment had no effect on initial cell attachment. To compare the effects of CXCL12's α, β, and γ isoforms on vessel behavior/morphology, each were introduced individually into vessel channels at a concentration of 100 ng/mL (Peprotech Inc.). For CD44 blocking experiments, trypsinized HUVECs were treated with medium containing CD44 antibody (2 μg/mL, Invitrogen) for 30 minutes at room temperature prior to seeding.

5.4 Quantification of ECM-bound CXCL12

6 mg/mL concentration of collagen-only ECM and collagen/HA were cast on the SPR chip (Nicoya technology) and polymerized overnight. CXCL12-α, β, and γ isoforms were added at a concentration of 100 ng/mL then incubated for 1 day. SPR measurements were conducted using the Nicoya LSPR instrument.

5.5 Sprouting angiogenesis assay

HUVECs were cultured in microfluidic devices for three days using culture medium supplemented with CXCL12 isoforms. Phase-contrast images of sprouts from ECM/vessel interfaces were taken every 24 hours and NIH ImageJ software was used to evaluate the specific sprouting area of each device. The Normalized Sprouting Percentage was defined in Equation 1, which is a percentage of sprouting area increase divided by a reference area A_{REF}. A(0) takes into account the area of any sprouts present before treatment while $A(N)$ represents total sprouting area N days after treatment begins. To analyze cases involving non-sprouting phenotypes, such as endothelium expansion into collagen/HA matrices, the total area of endothelium expanded into the ECM compartment but behind the monolayer was tracked over time and defined as vessel dilation (See supporting information Figure S2 and S3).

$$\text{Normalized Sprouting percentage } (\%) = \frac{A(N) - A(0)}{A_{REF}} \times 100\% \quad \text{Equation 1}$$

5.6 Apparent vessel permeability measurement

6 mg/mL collagen was used for permeability experiments to minimize spontaneous sprouting. HUVECs were cultured in the microfluidic devices for 2 days with individual CXCL12 isoform-supplemented medium prior to the permeability measurement. To measure the apparent permeability, 2 μL of 70 kDa Texas Red-conjugated Dextran fluorescent dye at a concentration of 0.05 mM was passively loaded into one of the HUVEC-lined channels. Time-lapse images of dye diffusion from the vessel channel into the ECM channel were taken with an epifluorescent microscope for at least 5 mins. NIH ImageJ software was used to analyze the intensity change over time in the adjacent ECM region as dye diffused across the endothelial monolayer. The apparent permeability P_{App} of each microvessel was calculated using Equation 2. ΔI is the constant source intensity in the vessel channel immediately outside of each aperture, $\frac{dI}{dt}$ is the intensity change in the adjacent ECM region over time, and $\frac{V_v}{S_v}$ is a volume to surface area ratio of the dye-loading channel.

Representative analytical images of an apparent permeability

$$P_{App} = \left(\frac{1}{\Delta I}\right) \times \left(\frac{dI}{dt}\right) \times \left(\frac{V_v}{S_v}\right). \quad \text{Equation 2}$$

measurement are provided in supporting information Figure S4.

5.7 Immunofluorescence staining

HUVECs that were cultured for 3 days in microvessel analogue system were fixed by 4 % paraformaldehyde (Sigma-Aldrich) for 15 minutes at room temperature. Then, the microvessels were permeablized by incubating with 0.1 % Triton X-100 (Sigma-Aldrich) for 20 minutes. Subsequently, the microvessels were incubated with 0.1% BSA overnight at 4 °C to avoid non-specific binding. VE-cadherin was stainned by incubationg with Alexa 647

conjugated anti-human VE-Cadherin primary antibody (Life Technologies) overnight. Cell nuclei of HUVECs were stainned by DAPI at 1:1000 dilution for 5 minutes. Confocal microscopy was performed on the stained microvessel using a laser scanning confocal microscope (Nikon A1R) with a 40X oil immersion objective. Confocal stacks of approximately 150 μm in height with a z-step of 0.5 μm were acquired for image analysis (~300 total images per stack). Reconstruction of the image stacks were done with Imaris software for the top and planar views.

5.8 Statistical analysis

Numerical data reported in this manuscript were expressed as mean ± the standard error (S.E.M). Each experimental condition was performed at least in three replicates to conduct statistical analysis. Variations of all data were statistically analyzed by performing one-way ANOVA followed by post-hoc unpaired, two-tailed Student t test, executed by origin lab software. To compare the statistical difference of each experimental condition, the asterisk mark (∗) was applied as ∗ for p-value <0.05, ∗∗ for p-value <0.01, and ∗∗∗ for p-value <0.001.

Supplementary Material

Refer to Web version on PubMed Central for supplementary material.

Acknowledgements

This work was supported by funding awarded to J.W.S. from an NSF CAREER Award (CBET-1752106), The American Heart Association (15SDG25480000), Pelotonia Junior Investigator Award, NHLBI (R01HL141941), and The Ohio State University Materials Research Seed Grant Program, funded by the Center for Emergent Materials, an NSF-MRSEC, grant DMR-1420451, the Center for Exploration of Novel Complex Materials, and the Institute for Materials Research. Partial personnel support through The Mark Foundation for Cancer Research (18–024-ASP) is also acknowledged. C.-W.C and A.A. gratefully acknowledge funding from the Pelotonia Graduate Fellowship Program. MC-M thanks the supports from an OSU Graduate Enrichment Fellowship and a Discovery Scholars Fellowship.

Reference

[1]. Carmeliet P, Jain RK, Nature 2011, 473, 298. [PubMed: 21593862]

[2]. a) Carmeliet P, Nature 2005, 438, 932; [PubMed: 16355210] b) Kerbel RS, N Engl J Med 2008, 358, 2039. [PubMed: 18463380]

[3]. a) Claesson-Welsh L, Ups J Med Sci 2015, 120, 135; [PubMed: 26220421] b) Nagy JA, Dvorak AM, Dvorak HF, Cold Spring Harb Perspect Med 2012, 2, a006544.

[4]. a) Dewhirst MW, Secomb TW, Nat Rev Cancer 2017, 17, 738; [PubMed: 29123246] b) Avendano A, Cortes-Medina M, Song JW, Front Bioeng Biotechnol 2019, 7, 6. [PubMed: 30761297]

[5]. Feng D, Nagy JA, Pyne K, Dvorak HF, Dvorak AM, J Exp Med 1998, 187, 903. [PubMed: 9500793]

[6]. Harney AS, Arwert EN, Entenberg D, Wang Y, Guo P, Qian BZ, Oktay MH, Pollard JW, Jones JG, Condeelis JS, Cancer Discov 2015, 5, 932. [PubMed: 26269515]

[7]. Dejana E, Orsenigo F, Lampugnani MG, J Cell Sci 2008, 121, 2115. [PubMed: 18565824]

[8]. Iozzo RV, San Antonio JD, J Clin Invest 2001, 108, 349. [PubMed: 11489925]

[9]. Hanahan D, Folkman J, Cell 1996, 86, 353. [PubMed: 8756718]

[10]. a) Hanahan D, Weinberg RA, Cell 2011, 144, 646; [PubMed: 21376230] b) Pietras K, Ostman A, Exp Cell Res 2010, 316, 1324. [PubMed: 20211171]

[11]. Toole BP, Nat Rev Cancer 2004, 4, 528. [PubMed: 15229478]

[12]. a) Feig C, Gopinathan A, Neesse A, Chan DS, Cook N, Tuveson DA, Clin Cancer Res 2012, 18, 4266; [PubMed: 22896693] b) Chanmee T, Ontong P, Itano N, Cancer Lett 2016, 375, 20; [PubMed: 26921785] c) Schwertfeger KL, Cowman MK, Telmer PG, Turley EA, McCarthy JB, Front Immunol 2015, 6, 236; [PubMed: 26106384] d) Theocharis AD, Tsara ME, Papageorgacopoulou N, Karavias DD, Theocharis DA, Bba-Mol Basis Dis 2000, 1502, 201.

[13]. DuFort CC, Paszek MJ, Weaver VM, Nat Rev Mol Cell Biol 2011, 12, 308. [PubMed: 21508987]

[14]. Bordeleau F, Mason BN, Lollis EM, Mazzola M, Zanotelli MR, Somasegar S, Califano JP, Montague C, LaValley DJ, Huynh J, Mencia-Trinchant N, Negron Abril YL, Hassane DC, Bonassar LJ, Butcher JT, Weiss RS, Reinhart-King CA, Proc Natl Acad Sci U S A 2017, 114, 492. [PubMed: 28034921]

[15]. Luker KE, Lewin SA, Mihalko LA, Schmidt BT, Winkler JS, Coggins NL, Thomas DG, Luker GD, Oncogene 2012, 31, 4750. [PubMed: 22266857]

[16]. Orimo A, Gupta PB, Sgroi DC, Arenzana-Seisdedos F, Delaunay T, Naeem R, Carey VJ, Richardson AL, Weinberg RA, Cell 2005, 121, 335. [PubMed: 15882617]

[17]. Ahirwar DK, Nasser MW, Ouseph MM, Elbaz M, Cuitino MC, Kladney RD, Varikuti S, Kaul K, Satoskar AR, Ramaswamy B, Zhang X, Ostrowski MC, Leone G, Ganju RK, Oncogene 2018, 37, 4428. [PubMed: 29720724]

[18]. a) Franchi A, Arganini L, Baroni G, Calzolari A, Capanna R, Campanacci D, Caldora P, Masi L, Brandi ML, Zampi G, The Journal of pathology 1998, 185, 284; [PubMed: 9771482] b) Guo P, Xu L, Pan S, Brekken RA, Yang ST, Whitaker GB, Nagane M, Thorpe PE, Rosenbaum JS, Huang HJS, Cavenee WK, Cheng SY, Cancer Res 2001, 61, 8569. [PubMed: 11731444]

[19]. Laguri C, Sadir R, Rueda P, Baleux F, Gans P, Arenzana-Seisdedos F, Lortat-Jacob H, PloS one 2007, 2, e1110.

[20]. Hardy D, Fefeu M, Besnard A, Briand D, Gasse P, Arenzana-Seisdedos F, Rocheteau P, Chretien F, Skelet Muscle 2019, 9, 25. [PubMed: 31533830]

[21]. Ray P, Stacer AC, Fenner J, Cavnar SP, Meguiar K, Brown M, Luker KE, Luker GD, Oncogene 2015, 34, 2043. [PubMed: 24909174]

[22]. a) Cavnar SP, Ray P, Moudgil P, Chang SL, Luker KE, Linderman JJ, Takayama S, Luker GD, Integr Biol-Uk 2014, 6, 564;b) Kojima T, Moraes C, Cavnar SP, Luker GD, Takayama S, Acta Biomater 2015, 13, 68. [PubMed: 25463502]

[23]. Song JW, Bazou D, Munn LL, Integr Biol-Uk 2012, 4, 857.

[24]. Kreger ST, Voytik-Harbin SL, Matrix Biol 2009, 28, 336. [PubMed: 19442729]

[25]. a) Netti PA, Berk DA, Swartz MA, Grodzinsky AJ, Jain RK, Cancer Res 2000, 60, 2497; [PubMed: 10811131] b) Wiig H, Aukland K, Tenstad O, Am J Physiol Heart Circ Physiol 2003, 284, H416.

[26]. Mohammadi H, Sahai E, Nat Cell Biol 2018, 20, 766. [PubMed: 29950570]

[27]. a) Cox TR, Erler JT, Dis Model Mech 2011, 4, 165; [PubMed: 21324931] b) Stylianopoulos T, J Biomech Eng 2017, 139.

[28]. a) Levett PA, Hutmacher DW, Malda J, Klein TJ, PLoS One 2014, 9, e113216;b) Voutouri C, Stylianopoulos T, PLoS One 2018, 13, e0193801.

[29]. Connell BJ, Sadir R, Baleux F, Laguri C, Kleman JP, Luo L, Arenzana-Seisdedos F, Lortat-Jacob H, Sci Signal 2016, 9, ra107.

[30]. Schasfoort RBM, in Handbook of Surface Plasmon Resonance, DOI: 10.1039/9781788010283-00060, The Royal Society of Chemistry 2017, p. 60.

[31]. Song JW, Munn LL, Proc Natl Acad Sci U S A 2011, 108, 15342. [PubMed: 21876168]

[32]. a) Jain RK, Science 2005, 307, 58; [PubMed: 15637262] b) R. K. Jain, 2005, 307, 58.

[33]. Dejana E, Orsenigo F, Lampugnani MG, Journal of Cell Science 2008, 121, 2115. [PubMed: 18565824]

[34]. Senbanjo LT, Chellaiah MA, Front Cell Dev Biol 2017, 5, 18. [PubMed: 28326306]

[35]. Flynn KM, Michaud M, Canosa S, Madri JA, Angiogenesis 2013, 16, 689. [PubMed: 23504212]

[36]. Teicher BA, Fricker SP, Clin Cancer Res 2010, 16, 2927. [PubMed: 20484021]

[37]. a) Hammer AM, Sizemore GM, Shukla VC, Avendano A, Sizemore ST, Chang JJ, Kladney RD, Cuitino MC, Thies KA, Verfurth Q, Chakravarti A, Yee LD, Leone G, Song JW, Ghadiali SN,

Ostrowski MC, Neoplasia 2017, 19, 496; [PubMed: 28501760] b) Nia HT, Liu H, Seano G, Datta M, Jones D, Rahbari N, Incio J, Chauhan VP, Jung K, Martin JD, Askoxylakis V, Padera TP, Fukumura D, Boucher Y, Hornicek FJ, Grodzinsky AJ, Baish JW, Munn LL, Jain RK, Nat Biomed Eng 2016, 1, 0004.

[38]. Liu M, Tolg C, Turley E, Front Immunol 2019, 10, 947. [PubMed: 31134064]

[39]. Auvinen P, Tammi R, Parkkinen J, Tammi M, Agren U, Johansson R, Hirvikoski P, Eskelinen M, Kosma VM, Am J Pathol 2000, 156, 529. [PubMed: 10666382]

[40]. a) Chauhan VP, Martin JD, Liu H, Lacorre DA, Jain SR, Kozin SV, Stylianopoulos T, Mousa AS, Han X, Adstamongkonkul P, Popovic Z, Huang P, Bawendi MG, Boucher Y, Jain RK, Nat Commun 2013, 4, 2516; [PubMed: 24084631] b) Duda DG, Kozin SV, Kirkpatrick ND, Xu L, Fukumura D, Jain RK, Clin Cancer Res 2011, 17, 2074; [PubMed: 21349998] c) Luker KE, Luker GD, Cancer Lett 2006, 238, 30. [PubMed: 16046252]

[41]. Lake SP, Hald ES, Barocas VH, J Biomed Mater Res A 2011, 99, 507. [PubMed: 21913316]

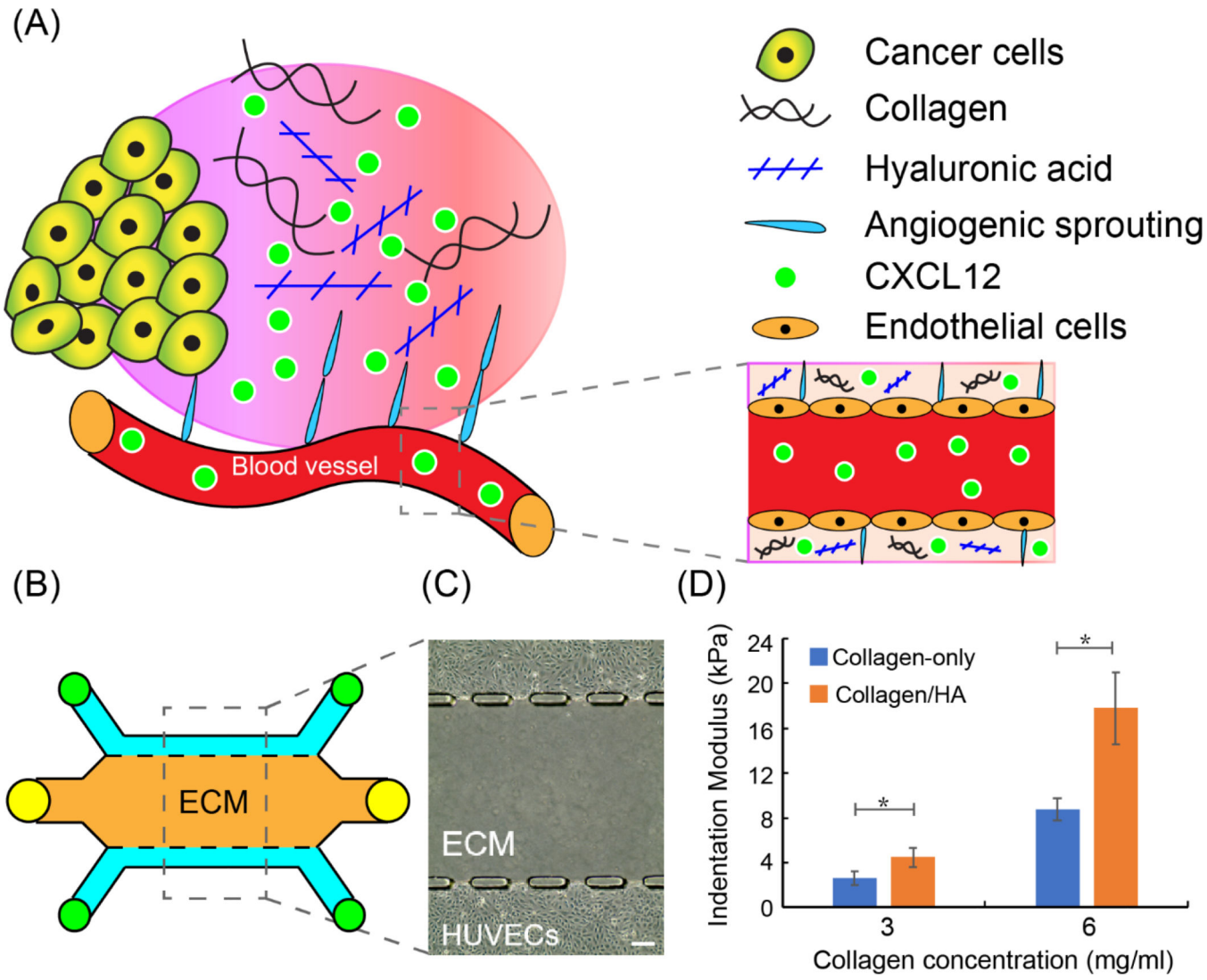

Figure 1.

3-D biomimetic model for studying vessel sprouting and permeability. (A) Schematic of CXCL12-induced tumor angiogenesis; (B) Schematic of developed microfluidic microvessel analogue for studying sprouting and permeability; (C) Phase-contrast images of human umbilical vein endothelial cells (HUVECs) cultured in microfluidic microvessel analogue. Scale bar = 100 μm; (D) Indentation modulus (stiffness) of collagen-only and collagen/HA matrices. The data were expressed as mean ± standard error (n=5 for collagen-only gel; n=7 for collagen/HA matrices). Unpaired two-samples t-test were performed to evaluate the statistical significance. * indicates p-value < 0.05.

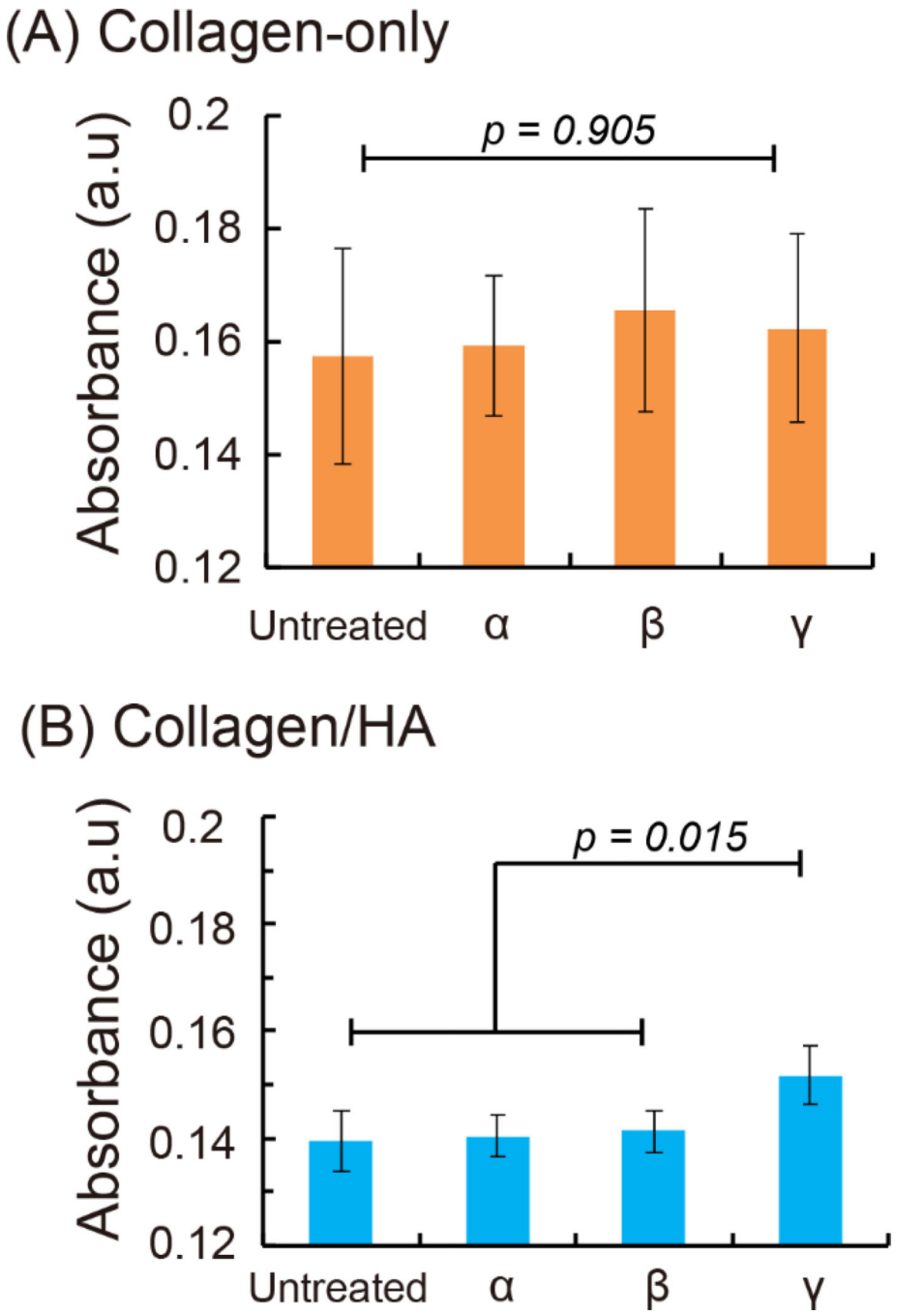

Figure 2.

CXCL12 isoform absorption on collagen-only and collagen/HA ECM measured by Surface Plasmon Resonance (SPR). (A) In the collagen-only ECM, CXCL12-α, β, and γ isoforms did not show preferentially absorption. (B) CXCL12-γ significantly increased 7 % compared to CXCL12-α and CXCL12-β isoforms on collagen/HA ECM. The data were expressed as mean ± standard error (n= 3). One-way ANOVA followed by post-hoc unpaired, two-tailed Student t test assays was performed to evaluate the statistical significance.

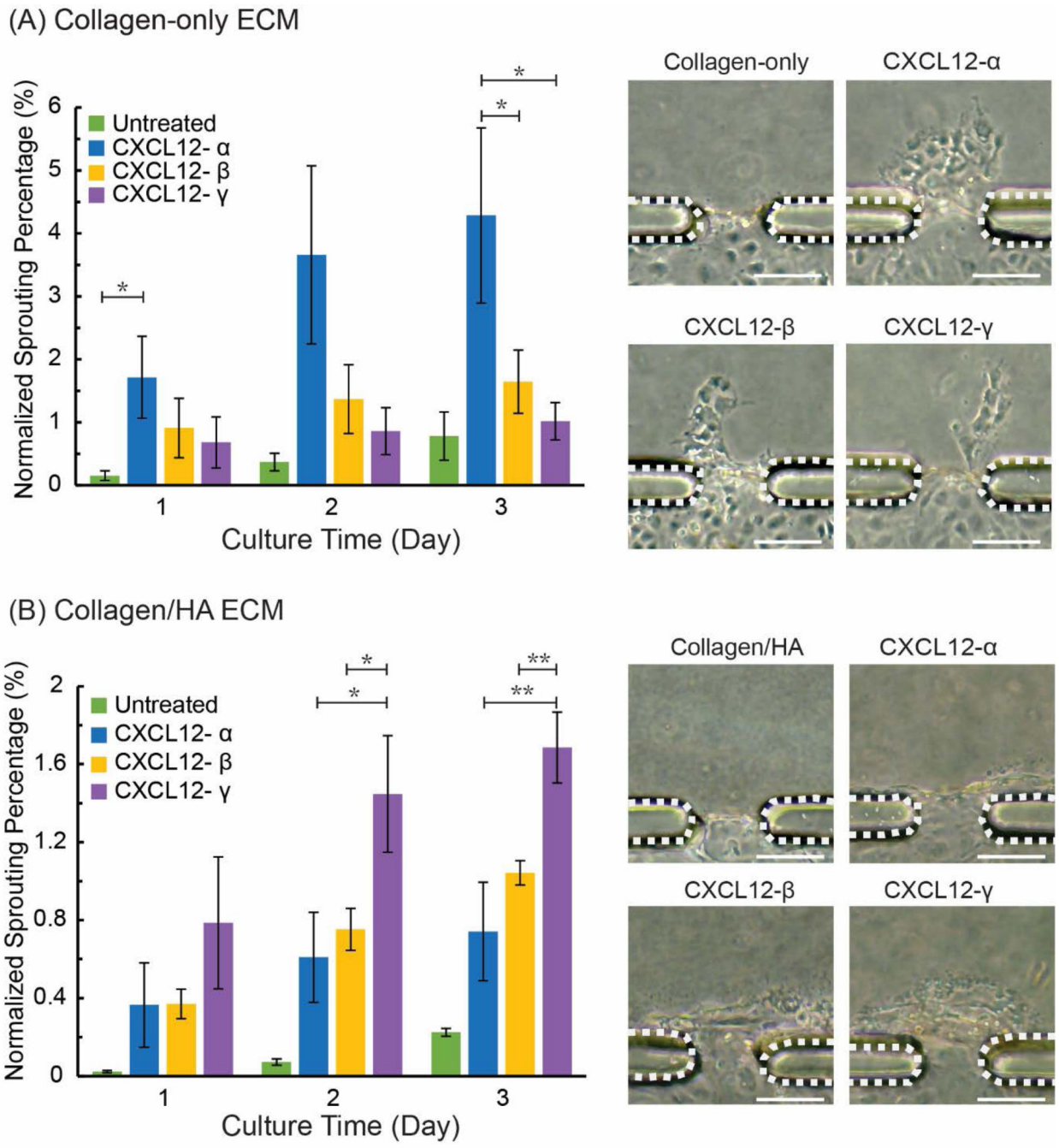

Figure 3.

Sprouting angiogenesis mediated by CXCL12 isoforms in collagen-only and collagen/HA matrices. (A) Sprouting ratio and sprouting morphology in collagen-only ECM; (B) Sprouting ratio and sprouting morphology in collagen/HA ECM. The data were expressed as mean ± standard error (n=4 for collagen-only gel; n=3 for collagen/HA matrices). Dashed lines indicate PDMS apertures. One-way ANOVA followed by post-hoc unpaired, two-tailed Student t test assays was performed to evaluate the statistical significance. * and ** indicate p-value < 0.05 and < 0.01, respectively. Scale bars = 100 μm.

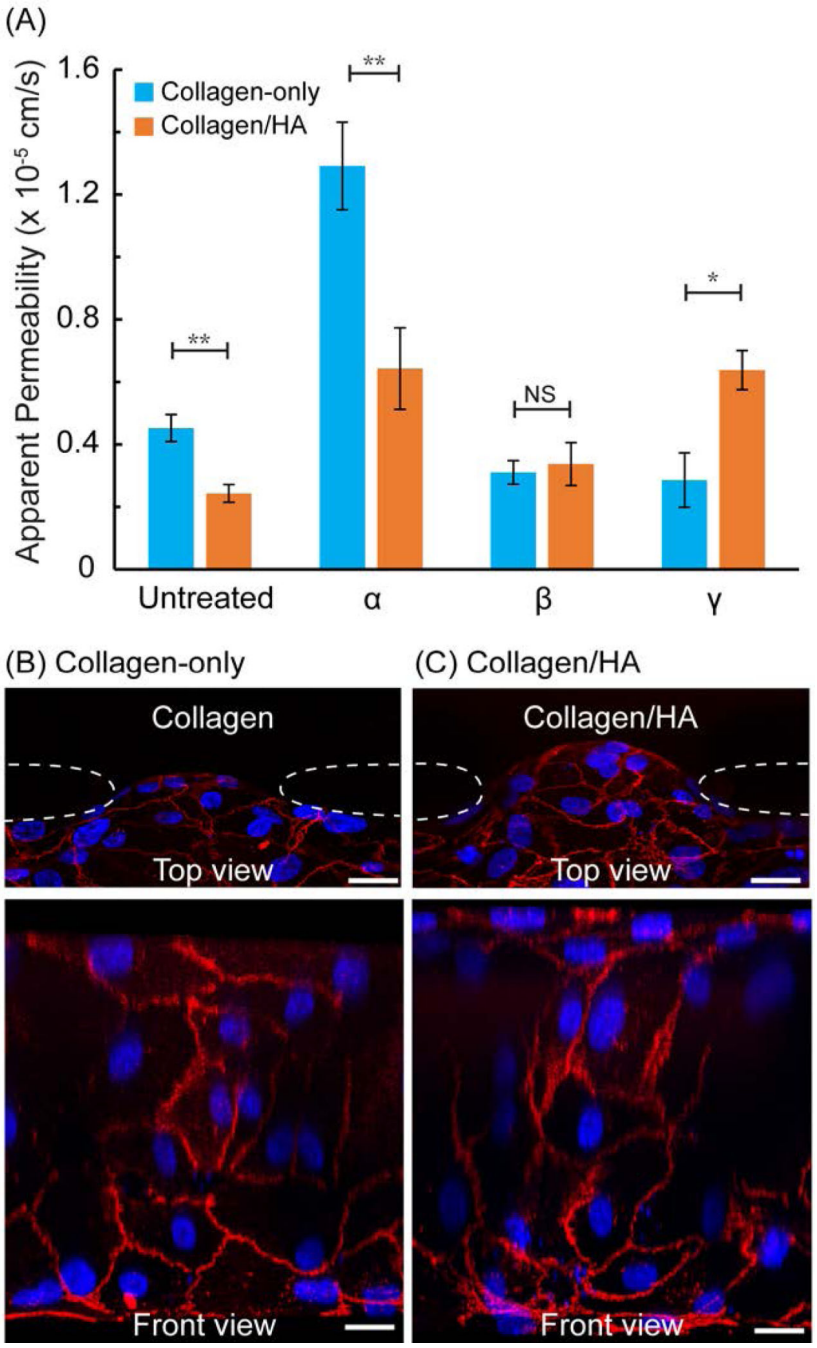

Figure 4.

(A) Apparent permeability of CXCL12 isoform treated microvessels in collagen-only and collagen/HA matrices; VE-cadherin junction protein (red) and DAPI (blue) staining of (B) untreated collagen-only and (C) untreated collagen/HA microvessel at the HUVEC/ECM interface. Dashed lines indicate PDMS apertures. Scale bars = 20 μm. The data were expressed as mean ± standard error (n=4 for collagen-only ECM test condition; n ≥ 3 for collagen/HA matrices condition). One-way ANOVA followed by post-hoc unpaired, two-

tailed Student t test assays was performed to evaluate the statistical significance. * and ** indicate p-value < 0.05 and < 0.01, respectively.

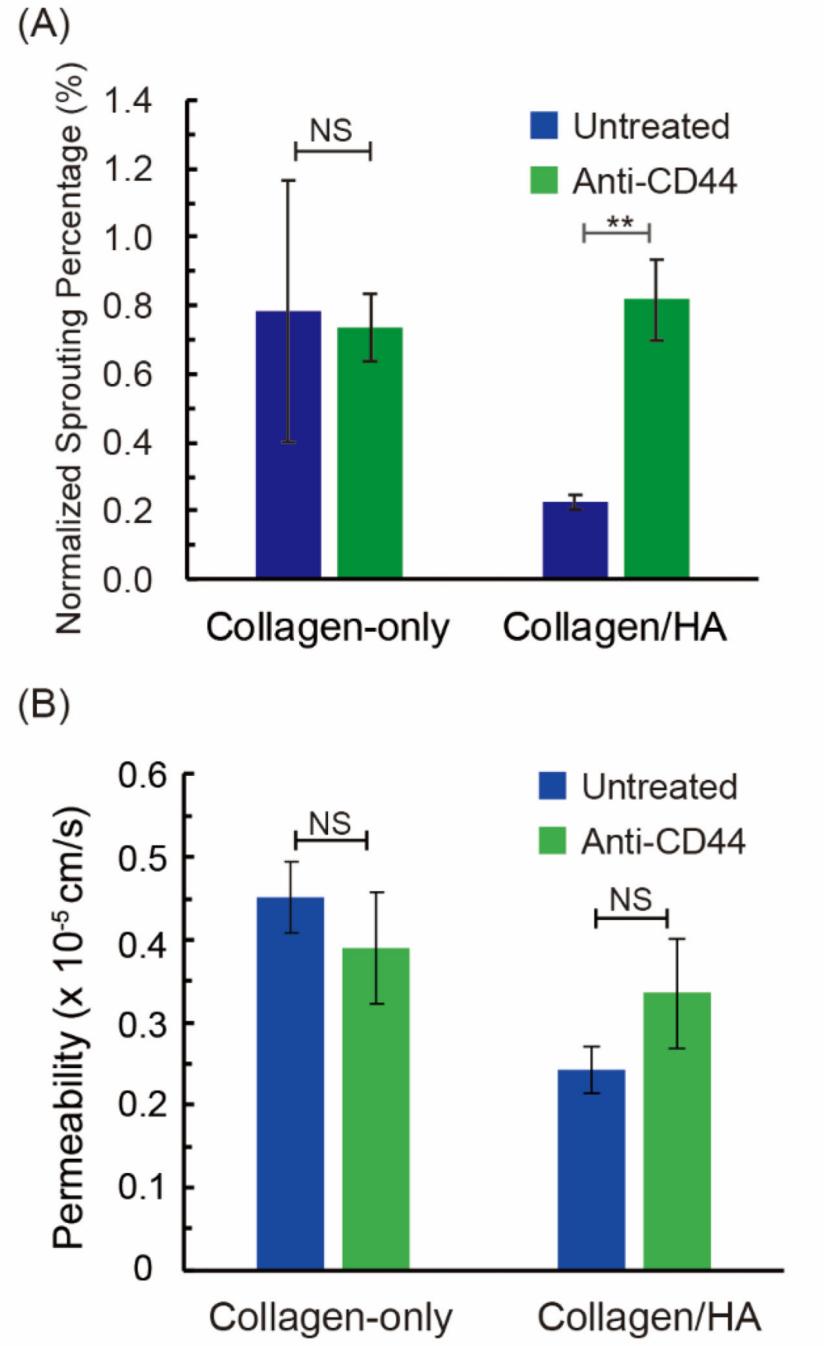

Figure 5.

HA-CD44 mediated sprouting and permeability. A blocking antibody (anti-CD44) was applied to neutralize ECM-located HA with CD44 receptors on HUVECs. (A) Vessel sprouting in collagen-only and collagen/HA matrices. For the collagen/HA ECM, anti-CD44 blocking significantly increased sprouting by 73% compared to the untreated control ($n \geq 3$ control unblocked experiments; $n \geq 5$ for CD44 functional blocking experiments). (B) Vessel permeability measurements in collagen-only and collagen/HA matrices. For the collagen/HA ECM, anti-CD44 increased permeability by 35% compared to untreated,

although this response was not statistically significant ($n \geq 3$ control unblocked experiments; $n = 7$ for CD44 functional blocking experiments). The data were expressed as mean ± standard error. Unpaired two-samples t test was performed to evaluate the statistical significance. NS indicates no significant difference.